JOURNAL OF GEOPHYSICAL RESEARCH, VOL. 100, NO. D11, PAGES 23,103–23,113, NOVEMBER 20, 1995

Atmospheric methane at Mauna Loa and Barrow observatories: Presentation and analysis of in situ measurements

Edward J. Dlugokencky,[1] L. Paul Steele,[2] Patricia M. Lang,[1] and Kenneth A. Masarie[1,3]

Abstract. In situ methane (CH_4) measurement techniques and data from the NOAA Climate Monitoring and Diagnostics Laboratory observatories at Mauna Loa, Hawaii, and Barrow, Alaska, are presented. For Mauna Loa, the data span the time period April 1987 to April 1994. At Barrow the measurements cover the period January 1986 to January 1994. Sixty air samples per day were measured with a fully automated gas chromatograph using flame ionization detection. Details of the experimental methods and procedures are given. Data are presented and assessed over various timescales. The average peak to peak seasonal cycle amplitudes obtained from four harmonics fitted to the detrended data were 25.1 ppb at Mauna Loa and 47.2 ppb at Barrow. When the seasonal cycle amplitude during each calendar year was determined as the difference between the maximum and minimum value from a smooth curve fitted to the data, the average amplitudes were (30.6 ± 4.2) ppb at Mauna Loa and (57.5 ± 11.4) ppb at Barrow. A discrepancy exists between these two methods due to the temporal variability in the positions of the seasonal maxima. The average trend at Mauna Loa was 9.7 ppb yr^{-1}, but this trend was observed to decrease at a rate of 1.5 ppb yr^{-2}. For Barrow the average trend was 8.5 ppb yr^{-1}, and the rate of decrease in the trend was 2.1 ppb yr^{-2}. At Mauna Loa, a diurnal cycle was sometimes observed with an amplitude of up to 10 ppb when averaged over 1 month.

Introduction

Methane plays an important role in the chemistry and radiative properties of the Earth's atmosphere (see review by *Cicerone and Oremland* [1988]). Its removal from the atmosphere is initiated by reaction with hydroxyl radical (HO)

$$HO + CH_4 \rightarrow CH_3 + H_2O \quad (1)$$

Reaction (1) is ultimately a source of carbon dioxide (CO_2; making a small indirect addition to CH_4's contribution as a greenhouse gas); affects the concentrations of HO and, through reactive nitrogen (NO_x) chemistry, ozone (O_3) in the troposphere; and is an important source of water vapor in the stratosphere. Reaction with a chlorine atom (Cl)

$$Cl + CH_4 \rightarrow HCl + CH_3 \quad (2)$$

is a termination step for the chlorine-catalyzed destruction of stratospheric ozone. Methane's strong IR absorption at 7.66 μm makes it the next most important contributor to radiative heating of the atmosphere after CO_2 and H_2O [*Mitchell*, 1989].

Measurements of CH_4 in the lower troposphere indicate that its atmospheric burden was increasing at ~0.7% yr^{-1} during the 1980s [e.g., *Steele et al.*, 1992]. Measurements of air trapped as bubbles in polar ice show that CH_4 increased from ~650 ppb (parts per 10^9, by volume) 300 years ago to about 1700 ppb today. Prior to industrialization, through glacial and interglacial periods, the CH_4 mixing ratio varied in the range 300-600 ppb [*Chappellaz et al.*, 1990].

Despite these important facts, the global budget of CH_4 is poorly understood. This is because CH_4 emissions from some individual sources (e.g., wetlands) vary by orders of magnitude over small spatial and temporal scales and they are spread over large geographical regions, so quantifying them directly with reasonable uncertainties is a difficult task (see *Fung et al.* [1991] for discussion). The NOAA Climate Monitoring and Diagnostics Laboratory (CMDL) has been monitoring atmospheric CH_4 with weekly air samples from an expanding number of sampling sites since 1983. These measurements have been used to study the CH_4 trend [*Steele et al.*, 1992; *Dlugokencky et al.*, 1994a,b], to constrain regional emissions of CH_4 [*Dlugokencky et al.*, 1993], and to constrain model studies of the global CH_4 budget [*Fung et al.*, 1991]. They also indicate that CH_4 is highly variable, particularly in the northern hemisphere. To understand this variability and its relationship to atmospheric CH_4 sources and sinks, the NOAA observatories at Mauna Loa, Hawaii (MLO), and Barrow, Alaska (BRW) were chosen as sites for quasi-continuous in situ measurements. Since the natural variation of atmospheric CH_4 in the background atmosphere is relatively small, measurement precision must be good.

The NOAA CMDL in situ measurements complement other CH_4 in situ measurement programs at Cape Grim,

[1]NOAA Climate Monitoring and Diagnostics Laboratory, R/E/CG1, 325 Broadway, Boulder, Colorado.

[2]CSIRO Division of Atmospheric Research, Mordialloc, Victoria, Australia.

[3]University of Colorado, Cooperative Institute for Research in Environmental Sciences, Boulder.

Copyright 1995 by the American Geophysical Union.

Paper number 95JDO2460.
0148-0227/95/95JD-02460$05.00

Australia [*Fraser et al.*, 1986]; Cape Point, South Africa [*Scheel et al.*, 1990]; Mace Head, Ireland, as part of the Global Atmospheric Gases Experiment (GAGE) and Advanced Global Atmospheric Gases Experiment (AGAGE) [e.g., *Simmonds and Derwent*, 1991]; the Japanese Antarctic Station, Syowa, Antarctica [*Aoki et al.*, 1992]; Cape Meares, Oregon [*Khalil et al.*, 1993], and Alert, NWT, Canada [*Worthy et al.*, 1994]. In situ measurements are used to understand trace gas budgets over local, regional, and larger spatial scales. Correlations among trace gas and aerosol species have been used in attempts to identify sources of arctic pollution [*Hansen et al.*, 1989; *Hopper et al.*, 1994]. Also, quasi-continuous measurements of CH_4 may be combined with meteorological data and air-mass trajectories to understand relationships between CH_4 emissions and temperature or precipitation. Finally, though we focus on CH_4 measurements made during background conditions, local CH_4 sources near in situ measurement sites may also be quantified from measurements during periods when the wind direction is from the source region.

Here we describe semicontinuous, in situ measurements of atmospheric CH_4 from the NOAA CMDL observatories at Mauna Loa, Hawaii, and Barrow, Alaska. Features in the data are examined that span timescales from one day (diurnal cycle) to the full time span of the records (seasonal cycles and trends). The measurements indicate that CH_4 at these sites is sometimes highly variable; although weekly, discrete air samples capture the gross features of the long-term trend and average seasonal cycle, semicontinuous, in situ measurements are necessary to understand this variability and its implications concerning CH_4 sources and sinks.

Experimental Procedures

Sampling Sites

Mauna Loa Observatory (19°32'N, 155°35'W) is located on the island of Hawaii, situated on the north side of Mauna Loa volcano (summit elevation 4170 m). It is at 3397 m, well above the height of the trade wind inversion [*Mendonca*, 1969], so it is well suited for making measurements of trace gases in the free troposphere. The observatory experiences a diurnal variation in wind regime. The early morning warming of the mountain causes upslope winds that bring air from below the inversion to the sampling site, typically from a northwesterly to northeasterly direction. As the upslope develops, temperature and relative humidity at the observatory increase. After sunset the mountain cools, and a downslope regime is established by ~2100 hours local time. Downslope drainage returns the site to cooler, drier conditions. Typically, downslope winds are from a southwesterly to southeasterly direction. These different wind regimes were considered during analysis of the CH_4 measurements.

Mauna Loa is an active volcano, so potential CH_4 emissions must be considered during periods of volcanic activity. During active periods, CO_2 is highly variable, even during downslope conditions. We have compared CH_4 data (T. Conway, unpublished data, 1994) with CO_2 data from a period ~7 months after the eruption of Mauna Loa in 1984. During periods of high CO_2 variability, CH_4 does not vary. Trace gas emissions from Mauna Loa have also been studied in detail by *Ryan* [1995], and CH_4 enhancements in the trace gas plume from the caldera were determined to be less than 1 ppb.

The Barrow Observatory (71°19'N, 156°36'W) is located on tundra, ~8 km northeast of Barrow, Alaska. Prevailing winds at the observatory are from the northeast, blowing off the Beaufort Sea. Air masses cross ~2 km of tundra before reaching the sampling site. Some strong anthropogenic CH_4 sources are within 10 km of the sampling site [*Bodhaine et al.*, 1981], including gas wells to the south, the town of Barrow to the southeast (population ~6000), and U.S. military installations to the north and northwest.

Gas Chromatography

Chromatographic conditions are summarized in Table 1. Methane was measured with a Carle (EG&G, Tulsa, Oklahoma) Series 400 gas chromatograph (GC). The GC contained a heated column oven (manufacturer states ±0.01°C control); internal 10-port and four-port, two-position GC valves (one of each); a heated nickel (Ni) catalyst; a microprocessor; and a flame ionization detector (FID). Our Carle GCs were built specifically for analysis of ambient levels of atmospheric CH_4, CO (carbon monoxide), and CO_2; CO and CO_2 were detected by FID after conversion to CH_4 on the Ni catalyst at 400°C in the presence of H_2 (hydrogen). The internal four-port valve was used to divert flows from either column to the Ni catalyst, then to the FID. Carbon monoxide and CO_2 measurements from the Carle GC are not reported. The CO measurements were used only as a

Table 1. Chromatographic Conditions for In Situ CH_4 Measurements

Site	Barrow	Mauna Loa
Precolumn	2.4 m × 0.3 cm OD 60/80 mesh silica gel	2.4 m × 0.3 cm OD 60/80 mesh silica gel
Analytical column	1.1 m × 0.3 cm OD 80/100 mesh molecular sieve 5A	1.1 m × 0.3 cm OD 80/100 mesh molecular sieve 5A
Column temperature, °C	86.4	88.5
Detector temperature, °C	86.4	88.5
Carrier gas (<0.5 ppm THC)	Zero grade He (99.995%)	Zero grade He (99.995%)
He flow rate at FID, mL min^{-1}	130	130
FID gases (<0.5 ppm THC)	Zero grade H_2 (≥99.99%) 40% O_2 in N_2 (certified mixture)	Zero grade H_2 (≥99.99%) 40% O_2 in N_2 (certified mixture)
Sample loop volume, mL	3	3

THC = total hydrocarbons

diagnostic, and CO_2 was monitored separately at each observatory with an infrared analyzer [*Thoning et al.*, 1989]. In situ CO measurements made by GC with a HgO reduction/resonance absorption detector were started at BRW in September 1991 and at MLO in May 1992. The Ni catalysts were removed from the Carle systems in February 1990 at BRW and in May 1990 at MLO.

The analysis sequence for CH_4 was as follows. Ambient air or reference gas was flushed through the sample loop at ~100 mL min^{-1} for 0.5 min. After a 10-s delay, which allowed the gas in the loop to relax to ambient pressure, the 10-port valve was switched, and the gas was injected onto the precolumn. The precolumn separated CO_2 from the analyte to prevent contamination of the analytical column by CO_2. After CH_4 was detected by the FID, the 10-port valve was switched back to the flush position; this reversed the order of the pre-column and analytical column in the flow sequence and prevented CO_2 from eluting onto the molecular sieve column.

The chromatographic method was modified at BRW in May 1992, so the precolumn is now backflushed to a vent. To achieve this, the plumbing configuration at the 10-port sampling valve was changed, and the valve is now returned to the flush position after CH_4 has eluted from the precolumn. This change, also planned for MLO, makes the remote analytical systems more robust, simplifies maintenance and repair, and provides the opportunity to shorten the analysis time.

Zero-grade He (helium) was further purified by passing it through a 2.5-cm OD by 50-cm-long stainless steel tube filled with a 1:1 mixture of molecular sieves 13X and 5A. Before their shipment from Boulder to the observatories, the He carrier gas and flame gases were checked for CH_4 contamination and rejected if found contaminated. This was necessary because we have found commercial cylinders of H_2 contaminated with up to 2 ppm CH_4. Such levels of impurity were unacceptable because they decreased the stability of the FID baseline signal and severely degraded the measurement precision.

Methane gas chromatographic peaks were quantified (in counts) using a Hewlett Packard (HP) 3393A programmable integrator. It integrated the 0-1 V signal from the GC electrometer with a sensitivity of 0.125 μVs per area count and 0.125 μV per height count. Quantification of the CH_4 peaks was based on peak height because the HP3393A combined with our integration method gave about a factor of 3 better precision than using peak areas [*Steele et al.*, 1987]. The lower limit to the precision of the CH_4 measurements was determined by the magnitude of the voltage delivered to the integrator from the electrometer and the resolution of the analog to digital (A/D) converter. The peak height for a 3 mL air sample with 1700 ppb was ~2.7 mV, and each increment of the 16 bit A/D used by the HP3393A was $1/2^{16}$ V, or 15.3 μV. This gives a theoretical limit to the resolution of the measurement of about 9 ppb. The observed precision was a factor of 3 better than this because of signal averaging by the integrator and because each aliquot of sample was referenced against the average of two aliquots of bracketing standard gas.

Integration of chromatographic peaks and reporting of raw chromatographic data were done with an integrator method: a collection of integrator operating parameters, which were varied during a chromatogram by a timetable, and report options. The operating parameters and timetable were optimized for precise detection of atmospheric CH_4. A report was generated for each aliquot injected, and storage and handling of the report were controlled by a BASIC program. Five aliquots were analyzed each hour; half were calibrated reference gas and half were air samples, for a total of 60 ambient air samples each day. The precision of any single CH_4 measurement, determined as the standard deviation (1σ) of 20 measurements of standard gas, was typically ~0.2%.

Sampling

One of four separate airstreams was supplied to the GC for analysis from a four-port Valco stream selection valve directed by an eight-position electric actuator. Actuator positions between valve ports were used as off (closed) positions. Two of the four ports were supplied with ambient air from the intake lines and two with calibrated reference gas teed off a single 0.16-cm OD line from the reference gas cylinder. Two similar, but separate, air intake lines were used to provide redundancy, robustness, and a means of quality control over the short and long term. Under background conditions, we expect the ambient CH_4 mixing ratio from both intake lines to agree within the measurement precision. If they did not agree, a sampling problem (usually a split diaphragm in the pump) was indicated. When a problem did occur with one of the lines, usually the other was unaffected, so periods of complete data loss were reduced. Using two intake lines also allowed us to evaluate the effect of aging intake tubing on the CH_4 mixing ratio by replacing one of the older lines with a new one, and comparing the measurements. The analysis sequence alternated between ambient air and reference gas, so each ambient sample was bracketed by aliquots of reference gas. The sample inlets were ~38 m above ground level at MLO and ~16 m at BRW. Dekabon tubing (Eaton Corp., Aurora, Ohio, consisting of a high-density polyethylene outside layer, an aluminum middle layer, and an ethylene copolymer inner coating) was used to conduct air from the sample inlets (inverted 500-mL stainless steel beakers) to the sample pumps. A pump with a butyl-rubber diaphragm (Cole Parmer Instrument Co., Chicago, Illinois, model 7530-40) was used to draw air through each sample line and supply it to the stream selection valve. A back pressure regulator maintained a constant pressure at the stream selection valve and insured continuous flushing of the sample line at about 8 L min^{-1} through a rotameter type flow meter. The back-pressure regulators were adjusted to keep the ambient air delivery pressure nearly identical to that of the reference gas (~40 kPa). In general, all aspects of the sampling and analysis system were configured to treat sample and standard gases identically, so any unforeseen problems would affect both gas streams equally [*Weiss*, 1981].

To eliminate variability in the CH_4 mixing ratio due to variations in humidity, the air (sample and reference gas) was dried by passing the gas from the stream selection valve through a Nafion tube (1.35 mm OD by 1.8-m length) contained in a leak-tight plexiglass cylinder filled with molecular sieve 13X [*Foulger and Simmonds*, 1979]. The Nafion tube was permeable only to H_2O vapor. Water was irreversibly trapped in the molecular sieve, and the air was dried to a dew point of about -35°C. The ends of the cylinder

were sealed with butyl O-rings. Once each year, the drying agent was replaced with a newly activated molecular sieve. The zeolite was activated by placing it in an open, flat container and heating it to 250°C for about 5 hours.

From the Nafion drier, the gas stream flowed through the sample loop, and then through about 1 m of 1.6-mm OD stainless steel tubing to a rotameter type flow meter where it was vented into the room. The measurement precision was partly a function of variations in the mass of air in the sample loop from one injection to the next, which was a function of the loop temperature and ambient pressure. Ambient pressure usually varied slowly, so it was ignored. The sample loop was inside the GC oven, which was stable to ±0.01°C, so sample temperature did not vary significantly from one run to the next.

Calibration

The working standards used at MLO since April 1987 and BRW since May 1987 were dry natural air stored in ACULIFE IV treated (a proprietary passivation process from Scott Specialty Gases, Plumsteadville, Pennsylvania) aluminum (Al) cylinders. (Prior to May 1987, two standards were used at BRW: one was a commercial mixture of CH_4 in synthetic air in an untreated Al cylinder, and the other was natural air in a steel cylinder.) The cylinders were filled with dry air at Niwot Ridge, Colorado, site C1 (~3020 m above sea level), to a pressure of 13.8 MPa with a Rix Industries (Oakland, California, model SA-3) compressor. Rix compressors use no oil or hydrocarbon lubricants which can affect the trace gas composition of the air. The site is remote and the compressor was operated away from buildings to prevent collection of contaminated air. We tried to ensure that the compressed air was representative of background conditions at Niwot Ridge, so contaminants could not affect the long-term stability of the reference gases or the chromatography.

The intake line to the pump was 1.27-cm OD Dekabon tubing fixed to a 10-m-tall mast. At the intake end, the tubing had a U-shaped bend with the opening pointing at the ground. A dust filter in a polyethylene beaker protected the pump from abrasive particles.

Without thorough drying of the air, the trace gas composition can rapidly change in ACULIFE IV treated cylinders. All air collected for use as reference was dried to <3 ppm H_2O (dewpoint ≈-70°C). The water content of the standards was checked using a Meeco Aquamatic (Meeco Instruments, Warrington, Pennsylvania), which had a detection limit for water of about 1 ppm. Phosphorous pentoxide (P_2O_5) on an inert support packed into 2.5-cm OD by 60-cm long stainless steel tubes with glass wool plugs at each end was used to dry the air. A 7-μm metal screen filter was placed before the cylinder as an added precaution to prevent particles from the drying tubes from entering it. The vapor pressure of P_2O_5 at normal working temperatures can be neglected (<10^{-13} Pa at 25°C). Two vertical tubes connected in series and positioned between the compressor and the cylinder were used for each cylinder. With this setup, some of the water was removed by the compression of the pump, which extended the useful life of the drying agent.

Each working standard was calibrated against the NOAA CMDL primary standard scale, which is traceable to the original reference gas cylinder purchased at the start of the program, and which has exhibited good long-term stability [see *Dlugokencky et al.*, 1994b]. Transfer of the standard scale was achieved with an estimated accuracy of ±0.2 ppb (95% confidence level). The absolute accuracy of the scale is unknown, but when it was compared to National Institute of Standards and Technology (NIST) CH_4 Standard Reference Materials (SRM), a relative difference of ~1.5% was observed, with CH_4 mixing ratios based on the NIST SRMs being higher.

Automation

Automation of the analytical system was controlled by the Carle GC microprocessor. The GC controller switched the internal GC valves and the external stream selection valve according to a timetable programmed into it, and it started the HP3393A integrator at the beginning of each run. The controller program repeated itself on a 12-min cycle.

Data acquisition from the analytical hardware was automated by a BASIC program run by the HP3393A integrator. The program accessed chromatographic reports to create the raw data files and customized hard-copy report, stored the raw data files to the data disk, and performed postrun calculations of the CH_4 mixing ratio in real time. Digitized peaks were not stored on the disk. The program plotted three of every 20 chromatograms for visual inspection of the chromatography. Real-time CH_4 mixing ratios were calculated from peak heights as the ratio of the ambient sample peak height to the average of the bracketing reference peaks, multiplied by the value of the CH_4 mixing ratio assigned to the reference gas. We have used eight gravimetrically prepared CH_4-in-air reference gases to verify that our detectors are linear in their peak height response to ±0.2% over the range 1000 to 2600 ppb.

Disks and chart rolls were replaced every 2 weeks and sent to Boulder for processing. The data were edited using a rule-based expert system [*Masarie et al.*, 1991] that identified with a "flag" all data obtained when the analytical system was not operating optimally. Less than 10% of the data were flagged due to unacceptable instrumental performance.

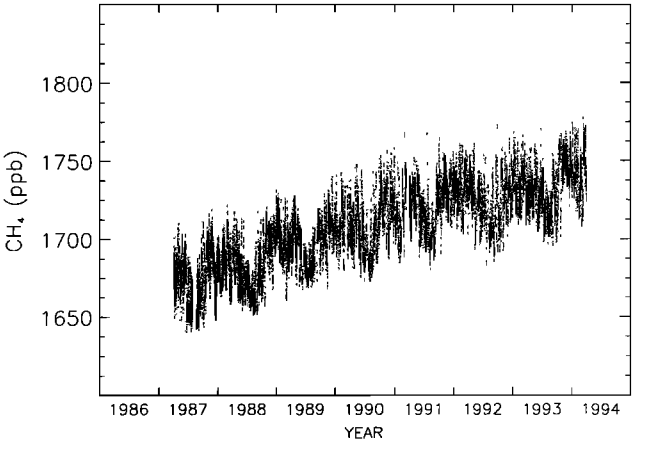

Figure 1. Hourly averaged CH_4 mixing ratios in ppb for Mauna Loa for the period April 2, 1987 to April 1, 1994. The data have been edited using a rule-based expert system to exclude measurements made when the analytical system was operating less than optimally. Typically, two to three measurements are averaged to give the hourly mean.

Results and Discussion

Edited, hourly averaged measurements of CH_4 mixing ratio in ppb, dry air are shown for Mauna Loa, Hawaii (Figure 1), and Barrow, Alaska (Figure 2a). Data from both sites are highly variable; temporal variations are discussed in more detail below.

Data Selection

We want to focus on trends and seasonal cycles which are representative of large, well-mixed volumes of the atmosphere; i.e., background conditions. At BRW, the time series is affected by local sources for certain wind directions, and MLO is affected by local meteorology. To constrain the time series to background conditions, the data are selected as described below.

Several strong CH_4 sources are located within 20 km of the Barrow Observatory, and this leads to a complex and highly variable record for certain wind directions (see Figure 2a). Our selection criteria for a clean air sector are wind direction within 020°-110° and wind speed ≥1 m s^{-1}. This excluded air masses coming directly from strong anthropogenic CH_4 sources in the vicinity of the observatory. In Figure 2b, the constrained BRW hourly averages are plotted; the prescribed conditions were in effect for at least 1 hour prior to inclusion of an hourly average. One hour was chosen to ensure that direct transport of local emissions to the station were excluded from the signal, without overconstraining the time series and flagging too many data. Varying this time period up to 5 hours had little effect on a visual inspection of the time series, except fewer data were retained. It is possible that local emissions could have been diluted and recirculated to the sampling site with changing wind direction. Possibly our best chance of detecting recirculated air would be with another tracer such as condensation nuclei. Note that when the wind direction and speed constraints are in affect for 1 hour prior to inclusion of a datum, the largest CH_4 values appearing in Figure 2a are no longer present in Figure 2b. At MLO, there are no local CH_4 sources that seem to affect the data.

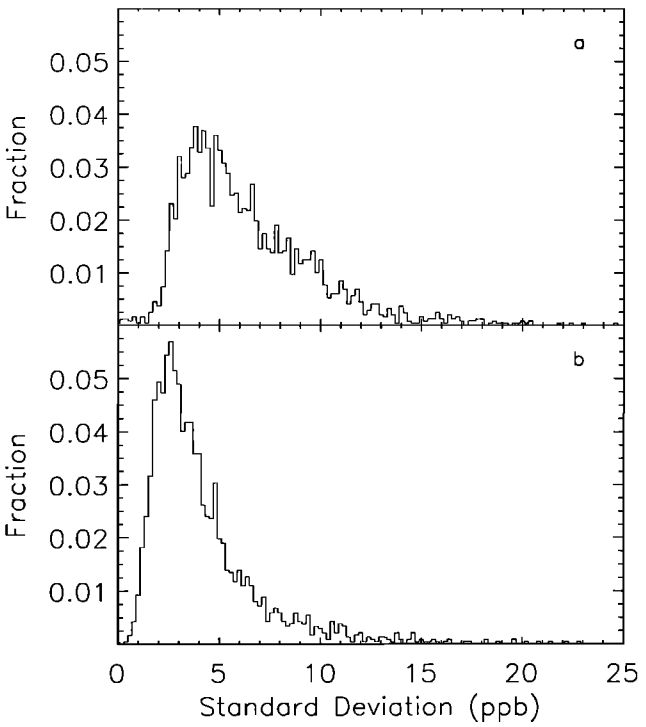

Figure 3. (a) Histogram of standard deviations for MLO daily means based on hourly averages. (b) Same as Figure 3a, but constrained to time periods between 0000 and 0700 local time to capture downslope conditions. In both cases, one daily mean has a single standard deviation lying outside the range plotted.

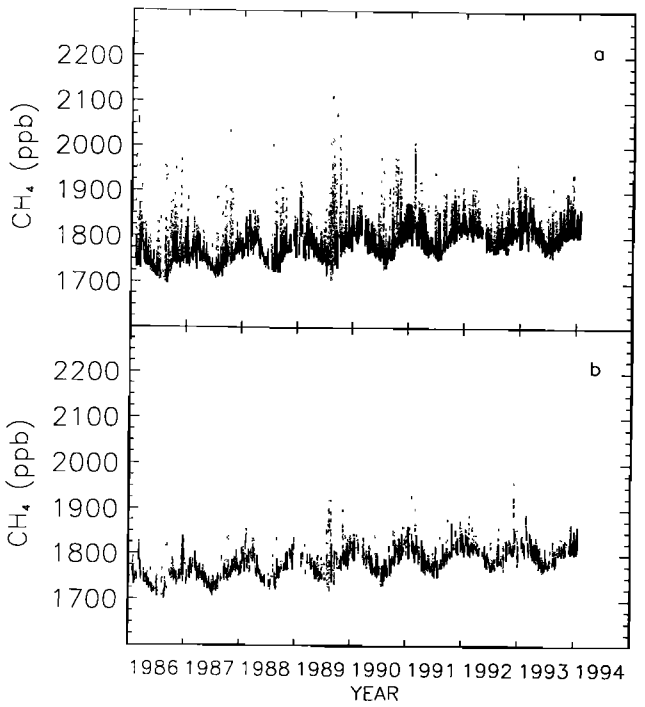

Figure 2. (a) Same as Figure 1, but for Barrow covering the period January 28, 1986 to January 27, 1994. (b) Same as Figure 2a, but wind direction within 020° to 110° and wind speed >1 m s^{-1} was required for 1 hour prior to inclusion of a datum.

Daily mean CH_4 mixing ratios provide suitable temporal resolution for determining trends and seasonal cycles, so these are calculated from the hourly averages described above. Distributions of the standard deviations from the daily mean calculations are shown for MLO in Figure 3a and BRW in Figure 4. Both distributions have relatively long tails, due to the natural variability of CH_4 at these sites. The distribution for MLO (Figure 3a) is skewed to the right when compared with BRW. The peak in the distribution for BRW at ~2.5 ppb is near the instrument precision. For MLO, the distribution peaks (Figure 3a) at ~4.5 ppb due to the variations associated with the upslope and downslope flow regimes. *Dlugokencky et al.* [1994b] found that CH_4 mixing ratios in the marine boundary layer determined from measurements of air samples collected at Cape Kumukahi (at sea level, ~80 km east of MLO) were on average ~1% greater than at MLO. In Figure 5a, monthly averaged deviations from the daily mean are shown ($\pm 1\sigma$) for each hour in the day at MLO for March 1992. A diurnal cycle is observed with an amplitude of ~10 ppb due to the movement of marine boundary layer air to the site during the daytime, upslope wind regime. Diurnal cycles were observed for some days in

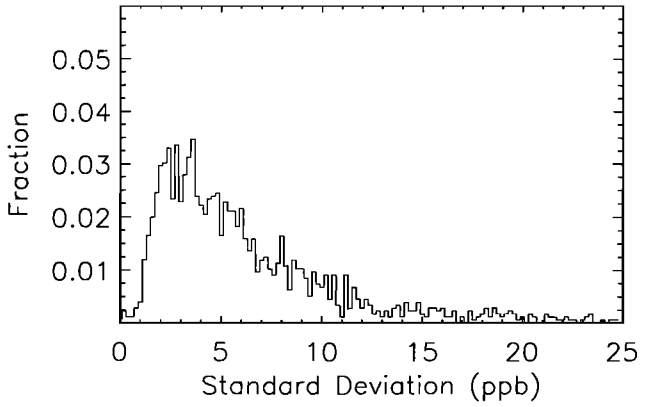

Figure 4. Same as Figure 3, but for Barrow. There were 49 (or 2.8%) standard deviations greater than the 25 ppb range plotted.

all months, but were not present every day, suggesting that the vertical CH_4 gradient between MLO and Cape Kumukahi was not always present or that strong upslope winds did not always develop. Deviations from the CH_4 daily mean value and dew point for March 1, 1992, are plotted in Figure 5b. On that day, the diurnal variation was ~45 ppb. When the MLO data are constrained to primarily downslope times (0000-0700 local time), the maximum in the standard deviation distribution occurs between 2 and 3 ppb, close to the instrument precision (Figure 3b). In the remainder of this study, we take advantage of the altitude at MLO to restrict our analysis to free tropospheric air masses. At BRW, diurnal cycles were not observed during any month. Daily averaged, constrained data are shown for MLO in Figure 6 and BRW in Figure 7.

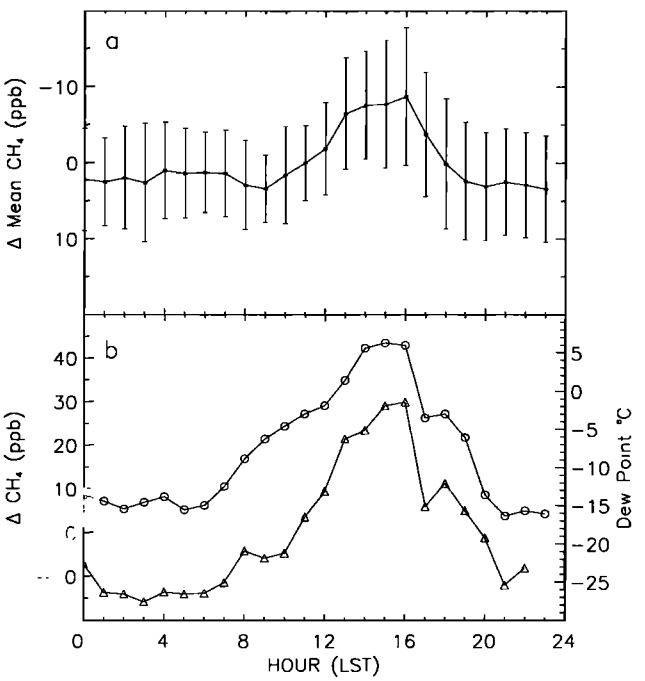

Figure 5. (a) Average deviations from the daily mean at Mauna Loa plotted by hour for March 1992. (b) Left scale: same as Figure 5a, but for March 1, 1992 (triangles). Right scale: hourly averaged dew point measurements for Mauna Loa on March 1, 1992 (circles).

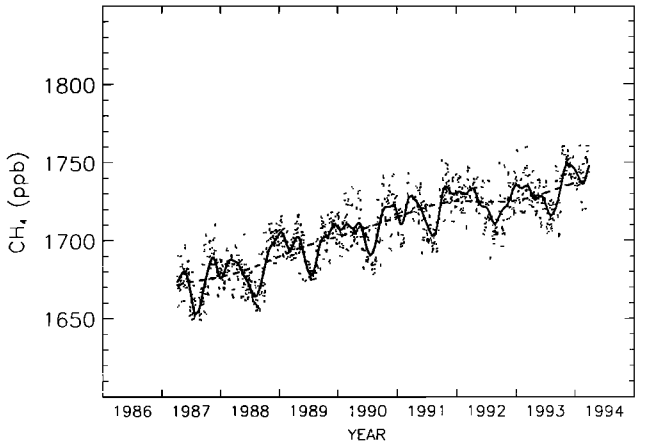

Figure 6. Daily mean CH_4 mixing ratios calculated from constrained data from Mauna Loa. The solid line is a smooth curve that has been fitted to the data. The dashed curve represents the deseasonalized, long-term trend. See text for details of the curve fits.

Tables of CH_4 mixing ratios are not included in this paper. Daily and monthly mean CH_4 mixing ratios calculated from NOAA CMDL in situ data are available from the Carbon Dioxide Information and Analysis Center (CDIAC, Oak Ridge, Tennessee; anonymous ftp to cdiac.esd.ornl.gov). Also, hourly, daily, and monthly mean CH_4 mixing ratios are available from the NOAA CMDL (NOAA CMDL, Boulder, Colorado; anonymous ftp to ftp.cmdl.noaa.gov).

Curve Fitting

A CH_4 time series is a combination of three primary factors: a long-term trend due to the small imbalance between CH_4 sources and sinks; an annual cycle due to the seasonality in atmospheric transport, some CH_4 sources, and the CH_4 photochemical sink; and short-term variations occurring on timescales of days to weeks due to variations in transport at the sampling sites. We separate these components for analysis by first fitting the data with a quadratic polynomial, which represents the long-term trend, and a series of four harmonics, which represents the average seasonal cycle:

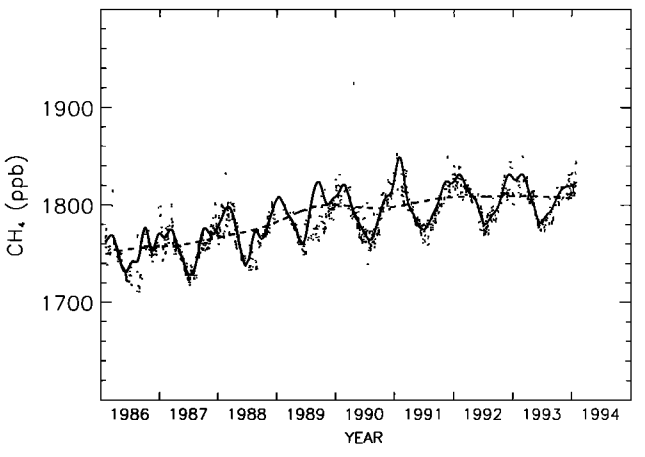

Figure 7. Same as Figure 6, but for Barrow.

$$f(t) = a_1 + a_2 t + a_3 t^2 + \sum_{i=1}^{4} [a_{2i+2} \sin(2\pi it) + a_{2i+3} \cos(2\pi it)] \quad (3)$$

Low-pass digital filtering of the residuals (after conversion to frequency domain) is applied to determine short-term variations (filter cutoff 4.56 cycles yr^{-1}) and interannual variations in the long-term trend (filter cut-off 0.55 cycles yr^{-1}) (see *Steele et al.* [1992] for details). The smooth curves in Figures 6 and 7 are a combination of equation (3) and the result of filtering the residuals with a filter cutoff frequency of 4.56 yr^{-1}.

Comparison With Flask Data

Our research group also makes measurements of atmospheric methane from discrete samples collected approximately weekly in Pyrex flasks from the CMDL Cooperative Air Sampling Network (sometimes referred to as "flask" samples) [*Dlugokencky et al.*, 1994b]. Mauna Loa and BRW are sites in the network. Relative precision of the discrete sample measurements has varied between ~0.1% (currently) and ~0.3% (at the start of the measurement program). Agreement between discrete samples and simultaneous in situ measurements was good. Figure 8 compares discrete flask data with hourly averaged in situ data for MLO and BRW. Average differences (±1σ) over the measurement periods were (0.0 ± 9.8) ppb at BRW and -(0.7 ± 5.0) at MLO. The in situ data were chosen to overlap with the hour in which the discrete sample was collected. At BRW, the largest differences shown in Figure 8b occurred at high CH_4 mixing ratios, presumably due to the higher within-hour variability observed during periods when CH_4 is elevated above background levels.

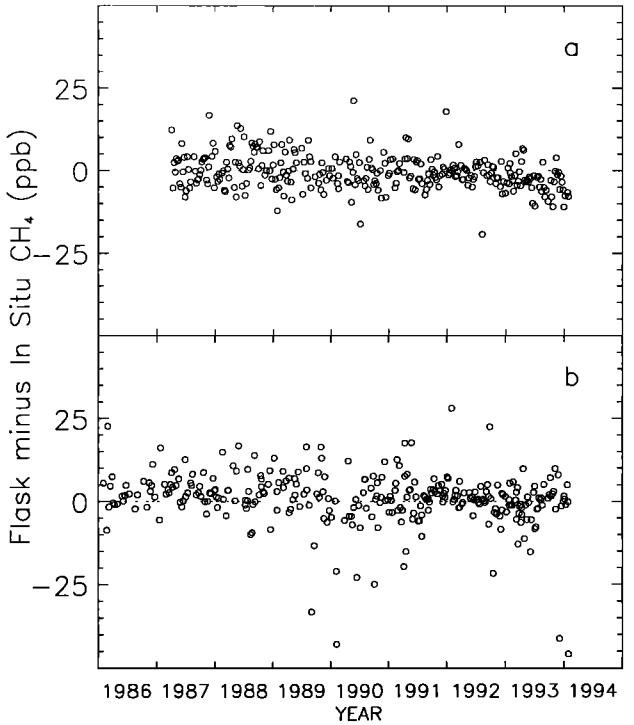

Figure 8. Comparison between CH_4 measurements in discrete samples and hourly averaged in situ data for (a) MLO and (b) BRW. The discrete sample data have been edited for quality control of the sampling and analysis procedures, and selected for background conditions [see *Dlugokencky et al.*, 1994b].

We have compared monthly mean CH_4 mixing ratios determined from in situ measurements and discrete samples, and they are in good agreement. In situ monthly means were calculated from evenly spaced, 1-day time steps extracted from the smooth curves fitted to the daily means (solid curves in figures 6 and 7). Monthly means determined from discrete samples were also calculated from smooth curves, but points were extracted at 1-week intervals. The smooth curves were used to ensure that the monthly means were not biased by unevenly spaced data and to capture slow variations in CH_4 as signal rather than noise. The average difference (±1σ), in situ minus discrete monthly mean, was (0.7 ± 4.4) ppb at MLO and (1.5 ± 9.7) ppb at BRW. Largest positive differences were 10 ppb in February 1993 at MLO and 38 ppb during September 1989 at BRW; largest negative differences were -9 ppb in November 1992 at MLO and -24 ppb in October 1986 at BRW. Due to the larger number of measurements used to calculate the monthly means with in situ data compared with discrete samples, the in situ monthly means are determined with more certainty. The standard deviations of the residuals (rsd) from the smooth curves fitted to the daily means in Figures 6 and 7 are 13 ppb for MLO and 18 ppb for BRW; smooth curves fitted to the measurements from discrete samples yield rsd's of 12 ppb for MLO and 13 ppb for BRW. The rsd is considered noise. This results in monthly means at MLO with an average uncertainty of ±2.5 ppb (standard error of the mean) from in situ measurements and ±6 ppb from discrete samples, and at BRW ±3.2 ppb from in situ measurements and ±6.5 ppb from discrete samples. The monthly means from discrete samples are determined with uncertainties that are small enough to define seasonal cycle amplitudes (~50 ppb in the high northern hemisphere) and long-term trends (~10 ppb yr^{-1}, averaged over a decade). The improved certainty in monthly means determined with in situ measurements is useful in determining the reliability of those features of the atmospheric CH_4 signal that are derived from discrete samples.

Seasonal Cycles

In Figure 9, average CH_4 seasonal cycles determined using two approaches are shown for the in situ measurements at MLO and BRW. Symbols were determined from detrended monthly means (i.e., January is the average of all Januarys, etc.). The uncertainties are ±1σ, and they give some estimate of the interannual variability in the shape of the seasonal cycle. Solid curves are composed of the fundamental and harmonic frequencies determined by equation (3); they represent the average seasonal cycles determined by the curve fitting process. The two approaches are in good agreement on the phase and amplitude of each average seasonal cycle. Average seasonal cycles are useful in constraining model studies of CH_4 sources and sinks, where transport is identical in each calender year [*Fung et al.*, 1991]. In practice though, the phase and amplitude of the cycle vary considerably from year to year. Our following discussion of the interannual variability in the CH_4 seasonal cycles is based on a comparison of the solid curves shown in Figures 6 and 7 with the average seasonal cycles shown in Figure 9.

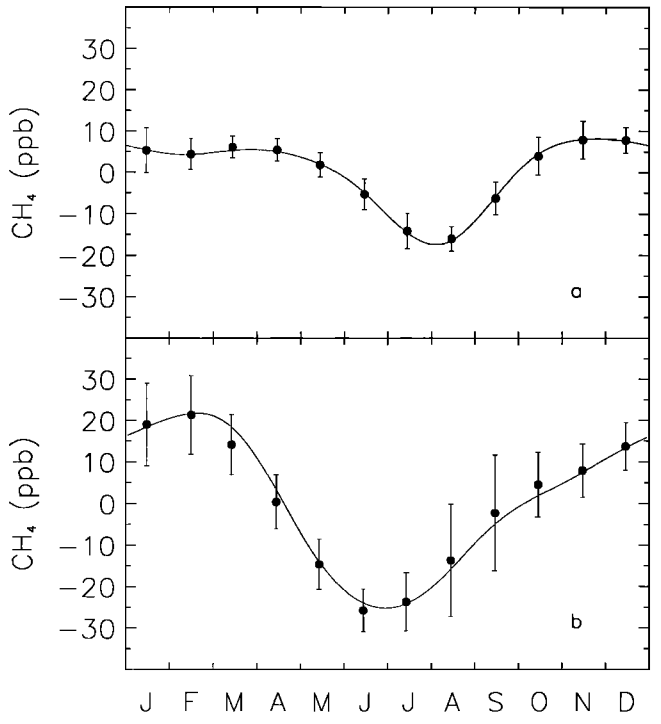

Figure 9. Average seasonal cycles for (a) Mauna Loa and (b) Barrow. Solid lines are the fundamental and harmonic frequencies determined by fitting equation (3) to the measurements. Average, detrended monthly means determined from the smooth curve fits to the data shown in Figures 6 and 7 are plotted as solid symbols. The error bars represent ±1 standard deviation.

At MLO, summer minima were observed from mid-July through mid-August, but the average position of the seasonal minimum occurred during the first week in August. Maxima in the curve fitted to the daily means were observed in each month from October through March (except February), but the average seasonal maximum was at the end of November. The peak-to-peak average seasonal cycle amplitude determined from the harmonics was 25.1 ppb; amplitudes determined from the smooth curve as the difference between maximum and minimum values within each calender year ranged from a low of 24 ppb to a high of 35 ppb, where the mean and standard deviation (1σ) were (30.6 ± 4.2) ppb. The latter value is ~20% larger than the amplitude determined from the harmonics because seasonal maxima were observed over a 6-month period, but they are averaged into a November maximum by the harmonic curve fitting process.

Harris et al. [1992] showed that atmospheric transport to MLO is largely responsible for the high CH_4 variability there, and it plays an important role in determining the CH_4 seasonal cycle. During July and August, the site is characterized by light, easterly flow off the Pacific Ocean. Air masses arriving at the observatory have not been in recent contact with strong CH_4 source regions, so CH_4 values are relatively low and exhibit little short-term variability. During October to May, alternation among different flow regimes leads to large variations in CH_4 mixing ratio. In particular, rapid transport from the Asian continent, a strong CH_4 source region, leads to periods when the maximum in the seasonal cycle is observed.

At BRW, the average position of the seasonal minimum, as determined by the smooth curve fitted to the constrained daily averages, was the end of June. Minima in the curve fit were observed from early June to early August. The average position of the seasonal maximum was at the beginning of February, but maxima were observed during October through March (except November). The average peak-to-peak seasonal cycle amplitude determined by equation (3) was 47.2 ppb. Amplitudes determined from the smooth curve ranged from 44 to 79 ppb, and the mean value was (57.5 ± 11.4) ppb.

General features in the CH_4 seasonal cycle at BRW can be explained qualitatively by considering the seasonality of CH_4 sources and sinks and the effects of Arctic meteorology. During winter, when the highest CH_4 mixing ratios are observed, the polar front is usually south of BRW. This, combined with a shallow mixed layer created by a relatively low inversion height, means that anthropogenic pollution emitted into the Arctic mixes into a relatively small volume of the atmosphere. The air is not diluted by air with low [CH_4] from aloft or low latitudes. During late August and early September, CH_4 emission rates peak for Boreal wetlands [*Fung et al.*, 1991], while the [HO] has already peaked and is starting to decline. This results in increased CH_4 mixing ratios observed at BRW. Methane mixing ratios decrease during March and April when the inversion breaks down, allowing dilution of northern air masses with air from upper levels [*Kahl*, 1990]. During late spring and summer, air masses with trajectories originating far to the south of BRW are more common [*Harris and Kahl*, 1994], the photochemical sink is more active, and CH_4 mixing ratios are considerably lower.

Comparing the two sites, the seasonal cycle minimum at BRW precedes MLO by about 6 weeks. This is due to the seasonality of CH_4 emissions from Boreal wetlands, which reach their peak emissions during late summer when soil temperature is highest, somewhat canceling the effect of chemical destruction. Although emissions from Boreal wetlands also play a role in determining the phase and amplitude of the CH_4 seasonal cycle at MLO, the observed effect is smaller because MLO is far from this source region.

A statistically significant trend in the amplitude of the CH_4 seasonal cycle due to the increasing burden of atmospheric CH_4 (since CH_4 destruction is proportional to [CH_4]) or possibly to a trend in [HO] was not found in either time series. Two methods were used to investigate this. In the first, the seasonal cycle amplitudes, determined as the difference between maximum and minimum values from the smooth curve fit for a given year, were fitted with a linear least squares line. A trend in the seasonal cycle amplitude of -(4.9 ± 2.0) % yr^{-1}, or -(1.5 ± 0.6) ppb yr^{-1} (n = 7, r^2 = 0.6) was determined for MLO and (1.9 ± 3.3) % yr^{-1}, or (1.1 ± 1.9) ppb yr^{-1} (n = 8, r^2 = 0.06) for BRW. In the second method, the CH_4 mixing ratios were fitted by the equation

$$g(t) = a_1 + a_2 t + a_3 t^2 + (1 + \alpha t) \times \sum_{i=1}^{2} [a_{2i+2}\sin(2\pi i t) + a_{2i+3}\cos(2\pi i t)] \quad (4)$$

The coefficient α is interpreted as a gain factor in the seasonal cycle amplitude, and t is time in years. We obtained the following values for α (in units of % yr^{-1}): BRW,

α = -(0.13 ± 0.06) and MLO, α = -(1.6 ± 0.1). Poor agreement between the two methods and the large uncertainties suggest that, due to the observed variability in CH_4 at the observatories, more years of measurements are necessary to determine if there is a significant trend in the seasonal cycle amplitude. This view is supported by our analysis of the seasonal cycle amplitudes from about 40 sites sampled weekly as part of the CMDL Cooperative Air Sampling Network [*Dlugokencky et al.*, 1994b]. Standard deviations of the year-to-year variations in the seasonal cycle amplitudes from 10 years of these discrete data were about ±10-20% for northern hemisphere sites and about ±7% for high-latitude southern sites.

Trends

Methane has been increasing at MLO and BRW over the periods of these measurements. The average rates of increase at each site were determined from the coefficient a_2 when a linear polynomial was used in equation (3). Changes in the growth rate were determined from $2a_3$, when the quadratic polynomial was used. Trends are summarized in Table 2. At MLO, the average rate of increase during the period April 1987 to April 1994 was 9.7 ppb yr^{-1}, but this rate was decreasing at 1.5 ppb yr^{-2}. At BRW, during the period January 1986 to January 1994, CH_4 increased at 8.5 ppb yr^{-1}, and the trend was decreasing by 2.1 ppb yr^{-2}.

For comparison, trends were also determined from discrete samples collected at BRW and MLO and from semi-hemispheric zonal means covering the same time periods as the in situ measurements, and these are included in Table 2. The zonal means were from the CMDL Cooperative Air Sampling Network [*Dlugokencky et al.*, 1994b]. Mauna Loa is compared with the zone from the equator to 30°N (low northern hemisphere, LNH) and BRW with the zone from 30° to 90°N (high northern hemisphere, HNH). While CH_4 mixing ratios from MLO are comparable to the LNH zone, those from BRW are ~30 ppb higher than the HNH zone. Also, *Dlugokencky et al.* [1994b] showed that CH_4 growth rates vary considerably among individual sites in the northern hemisphere, so more reliable estimates of the trend in the CH_4 burden are determined from zonal means. Despite this, agreement among trends and changes in trends shown in Table 2 for the quasi-continuous in situ measurements, discrete samples, and zonal means is reasonable. A 1 ppb yr^{-1} difference exists between trends derived from BRW in situ and discrete measurements. Since the trend is the derivative of the smoothed, deseasonalized time series, small differences between data sets are exaggerated when calculating trends. The slightly different trends calculated using in situ and discrete samples appear to be due to small differences between the data sets near the beginnings of the records (see Figure 8b). During 1986-1988, the average difference (±1σ) between flask and in situ hourly averages was (2.6 ± 7.7) ppb. Although this difference is not significantly different from zero, it reduces the estimate of the trend determined from discrete samples relative to the trend determined from in situ measurements. The reasons for the offset are unknown, but given the large natural variability at BRW, uncertainties in trends determined from single discrete sample records are expected to be reasonably large.

Table 2. Summary of Rates of Increase in Atmospheric CH_4 at MLO, BRW, and Semihemispheric Zonal Averages Determined From the CMDL Cooperative Air Sampling Network

Site	Trend, ppb yr^{-1}	ΔTrend, ppb yr^{-2}
MLO (In situ)	9.7	-1.5
MLO (Discrete)	9.2 ± 0.3*	-2.2 ± 0.3*
Equator-30°N (LNH)	9.1	-1.1
BRW (In situ)	8.5	-2.1
BRW (Discrete)	7.5 ± 0.5*	-1.9 ± 0.5*
30°-90°N (HNH)	8.9	-1.4

Time periods covered by the trends are April 1987 to April 1994 for MLO and LNH, and January 1986 to January 1994 for BRW and HNH.

*Uncertainties are determined from a nonparametric statistical technique (see text for details) and represent the uncertainty in the trends (Δ trends) due only to natural variability in CH_4 at the measurement sites. Uncertainties due to calibration and sampling errors are not included.

We assessed the uncertainties in trends determined from discrete samples using a nonparametric statistical method. Ten "fake" discrete sample time series were created by randomly selecting approximately one hourly average per week from the selected MLO and BRW in situ data sets, and then using equation (3) to determine trends from these fake records. For BRW the linear trends ranged from 7.9 to 9.3 ppb yr^{-1}, with a mean (±1σ) of (8.5 ± 0.5) ppb yr^{-1}, and at MLO the trends ranged from 9.2 to 10.3 with a mean (±1σ) of (9.6 ± 0.3) ppb yr^{-1}. These are reasonable estimates of the uncertainties in the trends due the natural variations in atmospheric CH_4 at the sampling sites. The added uncertainties in the trend due to sampling and calibration are difficult to quantify, but the small differences between trends determined from in situ and discrete records seem reasonable.

To further compare trends among in situ measurements, discrete samples, and zonal averages, instantaneous growth rates are plotted in Figure 10. The growth rates from in situ and flask data from MLO are compared with the LNH in Figure 10a, and BRW data are compared with the HNH in 10b. General features in these growth rates are similar; the rates of increase are largest in the early portions of the records, the growth rates are decreasing over time, and significant interannual variations in the growth rates exist. Mauna Loa represents the LNH better than BRW represents the HNH; this is likely due to the larger natural variability at BRW and the offset between BRW and HNH mixing ratios. The in situ and discrete sample growth rates diverge somewhat at the end of the BRW record in part due to end effects of the curve fitting process, which tend to exaggerate small differences between the data sets.

The CH_4 trend is due to a small annual imbalance (~6%) between CH_4 sources and sinks. Detailed information on temporal changes in CH_4 sources and sinks is unavailable, so the exact reasons for the positive but decreasing trend are unknown. Some possibilities for the decreased growth rate are increased atmospheric [HO], which increases the magnitude of the chemical sink [*Madronich and Granier*, 1992; *Prinn et al.*, 1992]; decreased growth in emissions, from cattle and other ruminant animals, and rice agriculture [*Khalil and Rasmussen*, 1993]; and decreased growth in

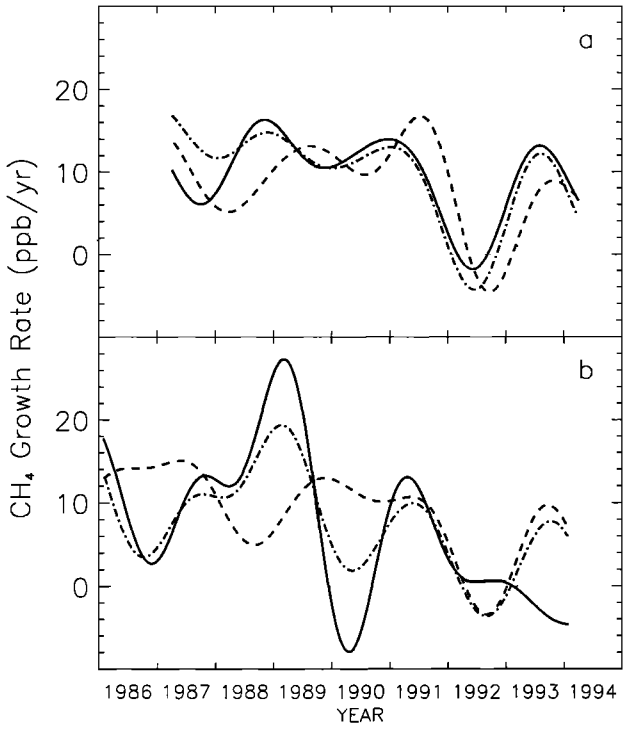

Figure 10. Instantaneous growth rate curves for (a) MLO and (b) BRW. The curves are determined as the derivative of the deseasonalized trend (dashed lines in Figures 6 and 7) fitted to each data set. Growth rates from in situ (solid lines), discrete samples (dot-dashed lines), and zonal means (dashed lines) are compared.

emissions from fossil fuel sources [*Steele et al.*, 1992; *Dlugokencky et al.*, 1994a,b].

Short-Term Variations

We have, so far, emphasized the gross features in the CH_4 records at BRW and MLO: features such as the long-term trend and seasonal cycle. But it is clear that the quasi-continuous measurements can reveal a greater understanding of the atmospheric CH_4 budget than discrete samples. The full range of information available from the quasi-continuous measurements is beyond the scope of this paper. Such detailed studies would likely require realistic models of three-dimensional transport, geographically distributed estimates of CH_4 sources and sinks, and, possibly, concurrent measurements of other amospheric trace species.

In anticipation of such studies, we draw attention to some obvious features in the quasi-continuous CH_4 records. At MLO, changes in CH_4 mixing ratio of 40-50 ppb occur suddenly, even during downslope conditions. Such changes are not associated with local meteorology, but rather, they reflect synoptic-scale variability, where large, regional-scale air masses have different CH_4 signatures. *Harris et al.* [1992] used isobaric trajectories and radon measurements from MLO to show that during winter, short-term variations result from alternation of different flow regimes. Strong westerly flow during winter rapidly transports air masses with high CH_4 mixing ratios from Asian source regions to MLO, while flow from tropical marine regions results in low CH_4 values. During summer, the degree of variability decreases due to the cessation of strong westerly flow from Asia, but transport resulting from motion around the north Pacific high can result in elevated CH_4 values due to transport from North America.

At BRW, rapid changes in CH_4 mixing ratios up to ~100 ppb were observed, even in air masses arriving from the clean air sector. The interpretation of such changes at BRW is more difficult than at MLO, since BRW is located near CH_4 sources (e.g., tundra wetlands), low-level and persistent inversions form which can trap emissions in a shallow surface layer, and the Arctic region is subject to long-range transport of pollution from lower latitudes during winter and spring [e.g., *Conway and Steele*, 1989]. An example of the value of quasi-continuous CH_4 measurements at BRW occurred in July 1989, when BRW experienced more than average southerly flow [*Harris and Kahl*, 1994] and temperatures there were 4.6°C above the long-term monthly mean. Direct measurements of CH_4 emissions from arctic tundra on the north slope of Alaska during August 1989 were more than a factor of 4 larger than in August 1987 [*Livingston and Morrissey*, 1991]. These higher emission rates offer a qualitative explanation for the persistent periods of high CH_4 mixing ratios observed at BRW during August 1989 (see Figure 7). This incident was not reliably captured in CH_4 measurements from discrete air samples collected at BRW.

Conclusions

The NOAA CMDL in situ CH_4 measurement systems have been used to determine the CH_4 mixing ratio in more than 150,000 aliquots of atmospheric air. The precision and relatively small amount of downtime provide useful measurements for interpreting variations in atmospheric CH_4 on synoptic and shorter time-scales [*Harris et al.*, 1992]. The major factor limiting the precision at this time is the relatively small sample volume. Future developmental efforts are focused on increasing the precision through larger sample size and improvements to the chromatography.

The in situ measurements provide insights into the nature of the variability in CH_4 at baseline observing sites in the northern hemisphere. They give us confidence that trends and seasonal cycles determined from weekly flask measurements are quantitatively correct, and that they are legitimate constraints on the global CH_4 budget. In this paper we have described the details of the CH_4 in situ measurements at MLO and BRW, and presented a qualitative analysis of features in the data. In future work, we will combine these measurements of CH_4 with concurrent in situ measurements of CO, CO_2, and meteorological variables, to make quantitative analyses of the regional and global budgets of these important trace gases.

Acknowledgments. We are indebted to the NOAA CMDL Observatory staff for their conscientious efforts in maintaining the CH_4 measurement instrumentation. In particular, we thank Alan Yoshinaga for help in the installation of the methane system at Mauna Loa, and to John Chin for his long-term dedication to its smooth operation. At Barrow, Dan Endres assisted in the installation of the original instrumentation, and has been an enthusiastic and dedicated supporter of the measurements over their full duration. Russ Martin was responsible for much of the development of the methane systems used at both observatories. We are grateful to Tom Conway and two anonymous reviewers for many useful comments on this manuscript.

References

Aoki, S., T. Nakazawa, S. Murayama, and S. Kawaguchi, Measurements of atmospheric methane at the Japanese Antarctic Station, Syowa, *Tellus, 44B*, 273-281, 1992.

Bodhaine, B.A., J.M. Harris, and G.A. Herbert, Aerosol light scattering and condensation nuclei measurements at Barrow, Alaska, *Atmos. Environ., 15*, 1375-1389, 1981.

Chappellaz, J., J.M. Barnola, D. Raynaud, Y.S. Korotkevich, and C. Lorius, Ice-core record of atmospheric methane over the past 160,000 years, *Nature, 345*, 127-131, 1990.

Cicerone, R.J., and R.S. Oremland, Biogeochemical aspects of atmospheric methane, *Global Biogeochem. Cycles, 2*, 299-327, 1988.

Conway, T.J., and L.P. Steele, Carbon dioxide and methane in the Arctic atmosphere, *J. Atmos. Chem., 9*, 81-99, 1989.

Dlugokencky, E.J., J.M. Harris, Y.S. Chung, P.P. Tans, and I. Fung, The relationship between the methane seasonal cycle and regional sources and sinks at Tae-ahn Peninsula, Korea, *Atmos. Environ., 27A*, 2115-2120, 1993.

Dlugokencky, E.J., K.A. Masarie, P.M. Lang, P.P. Tans, L.P. Steele, and E.G. Nisbet, A dramatic decrease in the growth rate of atmospheric methane in the northern hemisphere during 1992, *Geophys. Res. Lett., 21*, 45-48, 1994a.

Dlugokencky, E.J., L.P. Steele, P.M. Lang, and K.A. Masarie, The growth rate and distribution of atmospheric methane, *J. Geophys. Res., 99*, 17,021-17,043, 1994b.

Foulger, B.E., and P.G. Simmonds, Drier for field use in the determination of trace atmospheric gases, *Anal. Chem., 51*, 1089-1090, 1979.

Fraser, P.J., P. Hyson, R.A. Rasmussen, A.J. Crawford, and M.A.K. Khalil, Methane, carbon monoxide, and methylchloroform in the southern hemisphere, *J. Atmos. Chem., 4*, 3-42, 1986.

Fung, I., J. John, J. Lerner, E. Matthews, M. Prather, L.P. Steele, and P.J. Fraser, Three-dimensional model synthesis of the global methane cycle, *J. Geophys. Res., 96*, 13,033-13,065, 1991.

Hansen, A.D.A., T.J. Conway, L.P. Steele, B.A. Bodhaine, K.W. Thoning, P. Tans, and T. Novakov, Correlations among combustion effluent species at Barrow, Alaska: aerosol black carbon, carbon dioxide, and methane, *J. Atmos. Chem., 9*, 282-299, 1989.

Harris, J.M., and J.D.W. Kahl, Analysis of 10-day isentropic flow patterns for Barrow, Alaska: 1985-1992, *J. Geophys. Res., 99*, 25,845-25,855, 1994.

Harris, J.M., P.P. Tans, E.J. Dlugokencky, K.A. Masarie, P.M. Lang, S. Whittlestone, and L.P. Steele, Variations in atmospheric methane at Mauna Loa Observatory related to long-range transport, *J. Geophys. Res., 97*, 6003-6010, 1992.

Hopper, J.F., D.E.J. Worthy, L.A. Barrie, and N.B.A. Trivett, Atmospheric observations of aerosol black carbon, carbon dioxide, and methane in the high arctic, *Atmos. Environ., 28*, 3047-3054, 1994.

Kahl, J.D., Characteristics of the low-level temperature inversion along the Alaskan Arctic coast, *Int. J. Climatol., 10*, 537-548, 1990.

Khalil, M.A.K., and R.A. Rasmussen, Decreasing trend of methane: Unpredictability of future concentrations, *Chemosphere, 26*, 803-814, 1993.

Khalil, M.A.K., R.A. Rasmussen, and F. Moraes, Atmospheric methane at Cape Meares: Analysis of a high-resolution database and its environmental implications, *J. Geophys. Res., 98*, 14,753-14,770, 1993.

Livingston, G.P., and L.A. Morrissey, Methane emissions from Alaska arctic tundra in response to climate change, *Internationl Conference on the Role of Polar Regions in Global Change: Proceedings of a Conference Held June 11-15, 1990 at the University of Alaska Fairbanks*, vol. II, edited by G. Weller, C. Wilson, and B. Severin, pp. 372-377, Geophys. Inst. Univ. of Alaska, Fairbanks, 1991.

Madronich, S., and C. Granier, Impact of recent total ozone changes on tropospheric ozone photodissociation, hydroxyl radicals, and methane trends, *Geophys. Res. Lett., 19*, 465-467, 1992.

Masarie, K.A., L.P. Steele, and P.M. Lang, A rule-based expert system for evaluating the quality of long-term, in situ, gas chromatographic measurements of atmospheric methane, *NOAA Tech. Memo. ERL CMDL-3*, NOAA Environ. Res. Lab., Boulder, Colo., 1991.

Mendonca, B.G., Local wind circulation on the slopes of Mauna Loa, *J. Appl. Meterol., 8*, 533-541, 1969.

Mitchell, J.F.B., The "greenhouse" effect and climate, *Rev. Geophys., 27*, 115-139, 1989.

Prinn, R., D. Cunnold, P. Simmonds, F. Alyea, R. Boldi, A. Crawford, P. Fraser, D. Gutzler, D. Hartley, R. Rosen, and R. Rasmussen, Global average concentration and trend for hydroxyl radicals deduced from ALE/GAGE trichloroethane (methyl chloroform) data for 1978-1990, *J. Geophys. Res., 97*, 2445- 2461, 1992.

Ryan, S., Quiescent outgassing from Mauna Loa volcano, 1958-1994, in *Mauna Loa: A Decade Volcano, Geophys. Monogr. Ser.*, vol 92, edited by J.M. Rhodes and J.P. Lockwood, AGU, Washington, D.C., in press 1995.

Scheel, H.E., E.-G. Brunke, and W. Seiler, Trace gas measurements at the monitoring station Cape Point, South Africa, between 1978 and 1988, *J. Atmos. Chem., 11*, 197-210, 1990.

Simmonds, P.G., and R.G. Derwent, Measurements of ozone and other radiatively active gases at Mace Head in the Republic of Ireland, *Atmos. Environ., 25A*, 1795-1808, 1991.

Steele, L.P., P.J. Fraser, R.A. Rasmussen, M.A.K. Khalil, T.J. Conway, A.J. Crawford, R.H. Gammon, K.A. Masarie, and K.W. Thoning, The global distribution of methane in the troposphere, *J. Atmos. Chem., 5*, 125-171, 1987.

Steele, L.P., E.J. Dlugokencky, P.M. Lang, P.P. Tans, R.C. Martin, and K.A. Masarie, Slowing down of the global accumulation of atmospheric methane during the 1980's, *Nature, 358*, 313-316, 1992.

Thoning, K.W., P.P. Tans, and W.D. Komhyr, Atmospheric carbon dioxide at Mauna Loa Observatory, 2, Analysis of the NOAA GMCC data, 1974-1985, *J. Geophys. Res., 94*, 8549-8565, 1989.

Weiss, R.F., Determinations of carbon dioxide and methane by dual catalyst flame ionization chromatography and nitrous oxide by electron capture chromatography, *J. Chromatogr. Sci., 19*, 611-616, 1981.

Worthy, D.E.J., N.B.A. Trivett, J.F. Hopper, J.W. Bottenheim, and I. Levin, Analysis of long range transport events at Alert, NWT, during the polar sunrise experiment, *J. Geophys. Res., 99*, 25,329-25,344, 1994.

E.J. Dlugokencky, P.M. Lang, and K.A. Masarie, NOAA Climate Monitoring and Diagnostics Laboratory, R/E/CG1, 325 Broadway, Boulder, CO 80303.

L.P. Steele, CSIRO Division of Atmospheric Research, Private Bag 1, Mordialloc, Victoria 3195, Australia.

(Received March 22, 1995; revised August 4, 1995; accepted August 4, 1995.)